

Supporting Information for the Article

## Visible Light Mediated Metal-free Thiol-yne Click Reaction

**Sergey S. Zalesskiy, Nikita S. Shlapakov and Valentine P. Ananikov\***

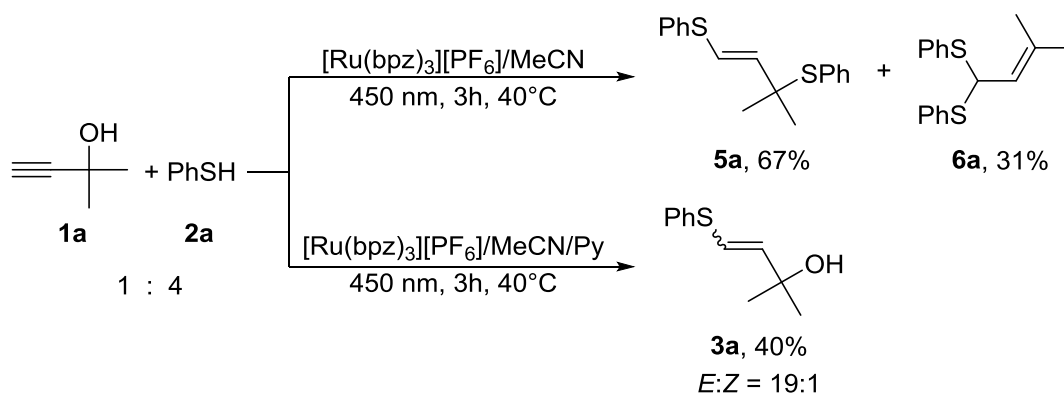
*Zelinsky Institute of Organic Chemistry, Russian Academy of Sciences, Leninsky prospekt, 47,  
Moscow, 119991, Russia; Fax: (+7) 499 1355328, E-mail: val@ioc.ac.ru; <http://AnanikovLab.ru>*

### Contents

S1. Optimization of reaction conditions .....	2
S2. Reactivity of different alkynes and steric effect.....	8
S3. Mechanistic studies of the visible light mediated thiol-yne click reaction .....	9
S4. Construction of a photochemical reactor using 3D printing .....	11
S5. Characterization of products 3a-p .....	14
References .....	31

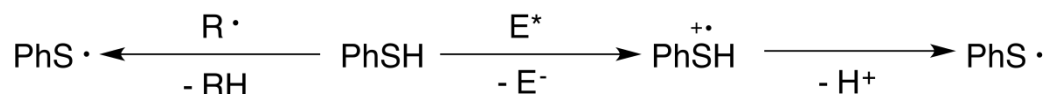
## S1. Optimization of reaction conditions

Initial reaction between the alkyne and thiol gave only side-products (**Scheme S1**, top route). To quench the undesired acid-catalyzed rearrangement pathway we have added a base to the studied system. Pyridine was found to be the base of choice, since common bases (with aliphatic CH<sub>2</sub> near the nitrogen atom) were rapidly oxidized under photochemical conditions. In the presence of pyridine the formation of by-products was suppressed and the desired sulfide was formed in 40% yield (**Scheme S1**, bottom route)



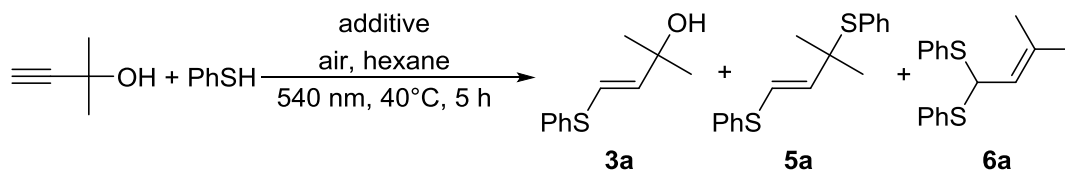
**Scheme S1.** Effect of pyridine in photoredox thiol-yne coupling.

The observed critical influence of pyridine on the reaction outcome can be explained by the following assumption. The formation of PhS<sup>•</sup> radicals may occur via two major routes: 1) homolytic H-abstraction from PhSH molecule (**Scheme S2**, left) or 2) single-electron transfer from PhSH to excited Eosin molecule (**Scheme S2**, right) via intermediate cation radical.



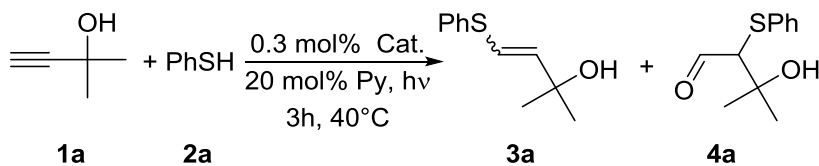
**Scheme S2.** Two pathways for the formation of PhS radicals.

The principal difference between the two routes is the accompanying release of H<sup>+</sup> during direct quenching of Eosin by PhSH which does not happen during the homolytic pathway. We demonstrated that the formation of by-products **5a** and **6a** is governed by the presence of protic acid in the system (**Table S1**, entries 1 and 2). Observation of these products under eosin-promoted conditions strongly evidences the increase of acidity in the system due to the formation of acidic cation-radicals. This fact suggests considerable contribution of direct Eosin-PhSH quenching to the generation of PhS radicals.

**Table S1.** Evaluation of radical formation pathways.

Entry	Additives (mol %)	Yield, %		
		3a	5a	6a
1	BEt <sub>3</sub> (25)	41	0	0
2	TsOH (20)	0	24	18
3	Eosin (0.3)	0	13	24
4	Eosin (0.3), Py (25)	85	0	0

To find optimal reaction conditions variation of photocatalysts and solvents were performed (**Table S2**). Several organic dyes were evaluated aiming to achieve the maximum alkyne conversion with good stereoselectivity. For organic dyes satisfactory results were achieved with Eosin Y.

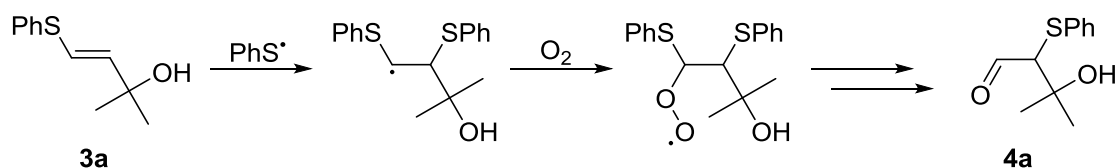
**Table S2.** Variations of photocatalysts and solvents.

Entry	Cat./solvent	Alkyne conversion, %	Yield, % <sup>a</sup>		
			3a ( <i>E:Z</i> )	4a	Unknown products
1	Fluorescein <sup>b</sup> /MeOH	95	60 (27:1)	15	20
2	Bengal Rose <sup>c</sup> /DMSO	48	40 (39:1)	2	6

3	Bengal Rose <sup>c</sup> /DMF	63	53 (25:1)	7	3
4	Bengal Rose <sup>c</sup> /Dioxane	55	44 (29:1)	4	7
5	Bengal Rose <sup>c</sup> /MeCN	9	2 (9:1)	2	5
6	Bengal Rose <sup>c</sup> /MeOH	37	28 (23:1)	2	7
7	Eosin Y <sup>c</sup> /DMSO	75	63 (30:1)	0	12
8	Eosin Y <sup>c</sup> /DMF	20	15 (14:1)	2	3
9	Eosin Y <sup>c</sup> /MeCN	85	56 (27:1)	19	10
10	Eosin Y <sup>c</sup> /MeOH	81	53 (25:1)	7	21
11	<b>Eosin Y<sup>c</sup>/MeNO<sub>2</sub></b>	<b>97</b>	<b>51 (30:1)</b>	<b>28</b>	<b>18</b>
12	Eosin Y <sup>c</sup> /Et <sub>2</sub> O	85	52 (20:1)	20	13
13	<b>Eosin Y<sup>c</sup>/Hexane</b>	<b>100</b>	<b>55 (25:1)</b>	<b>40</b>	<b>5</b>
14	Eosin Y <sup>c</sup> /without solvent	77	59 (49:1)	6	12
15	[Ru(bpz) <sub>3</sub> ][PF <sub>6</sub> ] <sup>b</sup> /MeCN	46	34 (20:1)	7	5

<sup>a</sup> Determined by NMR; <sup>b</sup> LED light 450 nm; <sup>c</sup> LED light 540 nm.

The formation of **4a** was reported previously for the electrochemical oxygenation of sulfides.<sup>1</sup> The authors proposed the mechanism based on the interaction of **3a** with thiolate radical followed by capture of the oxygen molecule (Scheme S3). From the mechanism it was evident that the key factors responsible for the formation of **4a** are the excess of PhSH and oxygen in the reaction mixture. We have found that the formation of **4a** in the studied system can be suppressed by tuning the **1:2** ratio and carefully controlling the amount of solvent, thus limiting the concentration of the dissolved oxygen (**Table S3**).

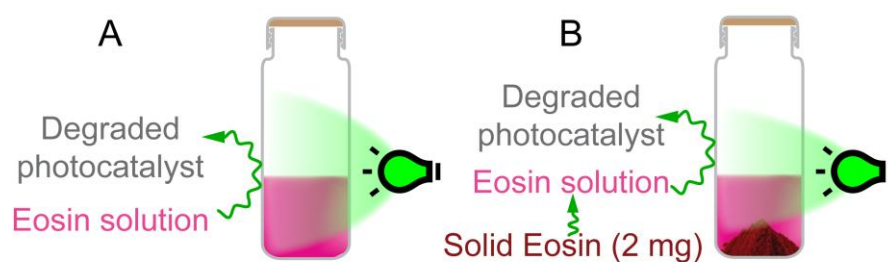


**Scheme S3.** Possible mechanism for the formation of **4a**.<sup>1</sup>

**Table S3.** Optimization of reagents ratio and amount of solvent.

Entry	<b>1a:2a</b>	Conditions	Yield, %		
			<b>3a</b> ( <i>E:Z</i> )	<b>4a</b>	Other by-products
1	1:2	E (0.05%), DMSO (500 μl), Py (20%), air, 2 h	17 (16:1)	1	0
2	1:2	E (0.3%), hexane (500 μl), Py (20%), air, 2 h	51 (25:1)	3	3
3	1:2	E (0.3%), hexane (500 μl), Py (20%), Ar, 2 h	14 (13:1)	0	0
4	1:1	E (0.3%), hexane (500 μl), Py (20%), air, 2 h	70 (26:1)	6	4
5	1:1	E (0.3%), hexane (500 μl), Py (20%), air, 5 h	77 (28:1)	13	7
6	1:1	E (0.3%), hexane (250 μl), Py (20%), air, 5 h	80 (30:1)	3	5
7	1:1	E (0.3%), hexane (250 μl), Py (25%), air, 5 h	81 (30:1)	3	1
8	1:1.1	E (0.3%), hexane (250 μl), Py (25%), air, 5 h	85 (50:1)	3	12

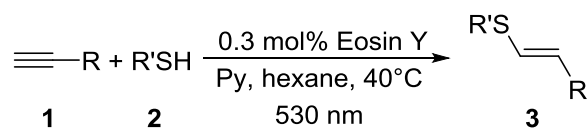
Another crucial role of the solvent nature was discovered during the studies of photocatalyst degradation. Reaction mixture containing Eosin Y underwent photo degradation of the catalyst, which was evident also from discoloration of the solution (**Figure S1, A**). The system in hexane with partially soluble Eosin Y (limited by solubility of the dye) maintained constant concentration of the photocatalyst and dramatically improved the yields (**Figure S1, B**).

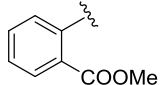


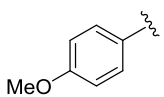
**Figure S1.** Photocatalyst degradation with completely soluble dye (A) and “saturation feedback” catalyst renewal with partially insoluble dye (B).

We have also performed several sets of control experiments in order to confirm that a real photocatalytic effect was observed in the studied system. Four sets of substrates were tested against different experimental conditions, including reactions in dark and reactions without photocatalyst (**Table S4**). It was found that in the absence of either light or photosensitizer small yields of **3** and poor stereoselectivity were observed.

**Table S4.** Control experiments for the study of photocatalytic effect.<sup>a</sup>



R	R'	Eosin Y	Light	Yield of <b>3</b> , %	<i>E</i> : <i>Z</i>
	Ph	+	+	85	50:1
		-	+	3	7:1
		+	-	2	6:1
		-	-	2	6:1
	Ph	+	+	89	40:1
		-	+	4	4:1
		+	-	2	1:1
		-	-	2	1:1
		+	+	97	35:1
		-	+	3	1:5
		+	-	1	1:3

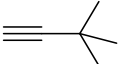
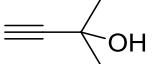
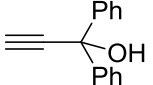
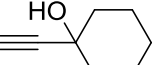
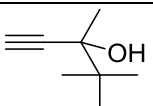
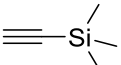
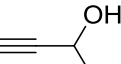
		-	-	1	1:3
		+	+	92	25:1
		-	+	19	18:1
		+	-	2	10:1
		-	-	2	10:1

<sup>a</sup> At low conversions *E/Z* ratio was roughly estimated from the NMR data.

## S2. Reactivity of different alkynes and steric effect

Selection of the alkynes illustrates plausible steric effect on the selectivity of the reaction. Bulk substituents provided a high selectivity in the studied thiol-yne click reaction (**Table S5**, entries 1-6), whereas reaction of less sterically hindered alkynes gave lower selectivity (entry 7) and it was not selective in the case alkynes with unsubstituted  $\alpha$ -carbon atom (entries 8-9). Accordingly, depending on the alkyne, a slower reaction with higher selectivity and faster reaction with lower selectivity were observed as reflected by reaction time: 1 h for entry 9, 2 h for entry 8 and 5 h for entries 1 – 7.

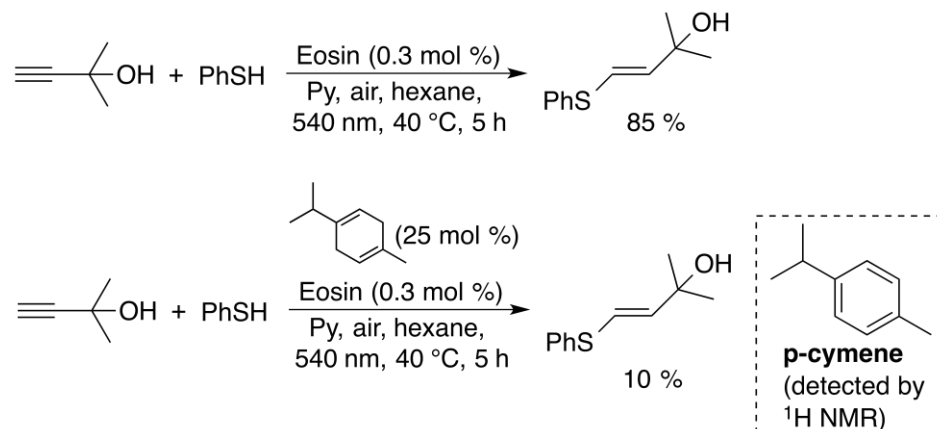
**Table S5.** Yields and selectivity in the catalytic addition reaction with different alkynes.<sup>a,b</sup>

Entry	Alkyne	Yield and E/Z selectivity
1		92% (99:1)
2		85% (50:1)
3		96% (40:1)
4		89% (40:1)
5		97% (35:1)
6		79% (25:1)
7		45% (4:1)
8		82% (1:1)
9		87% (1:1)

<sup>a</sup> See experimental part for the conditions. Reaction time: 5 h for entries 1 – 7, 2 h for entry 8 and 1 h for entry 9. <sup>b</sup> Trace amounts of double addition products were observed in some cases.

### S3. Mechanistic studies of the visible light mediated thiol-yne click reaction

To confirm radical nature of the studied process a control experiment with addition of  $\gamma$ -terpinene as a radical trap was carried out. Indeed, the reaction was suppressed and the product yield was decreased from 85% to 10% (**Scheme S4**). Involvement of radicals also initiated expected transformation of  $\gamma$ -terpinene to *p*-cymene as detected by NMR.



**Scheme S4.** Suppression of the reaction by addition of radical trap ( $\gamma$ -terpinene).

Formation of  $\text{PhS}\cdot$  radicals can be also demonstrated in the reaction without alkyne. In the absence of the alkyne recombination of the radicals resulted in the formation of the corresponding disulfide  $\text{PhS-SPh}$ . Although a high yield of the process is not expected, it should be sufficient for the measurements. Indeed, under studied conditions at 40 °C formation of  $\text{Ph}_2\text{S}_2$  was not detected in the absence of Eosin independently on the presence of air (**Table S6**, entries 1, 2). Small amount of  $\text{Ph}_2\text{S}_2$  was detected in the presence of Eosin (**Table S6**, entry 3), while regeneration of the dye in the presence of air resulted in the larger yield of  $\text{Ph}_2\text{S}_2$  (**Table S6**, entry 4).

**Table S6.** Formation of  $\text{Ph}_2\text{S}_2$  in the photochemical transformation of  $\text{PhSH}$  without alkyne.<sup>a</sup>

Entry	Conditions	Yield of $\text{Ph}_2\text{S}_2$ , %
1	Without Eosin and without air	ND
2	Without Eosin and with air	ND
3	With Eosin and without air	3
4	With Eosin and with air	16

<sup>a</sup> Conditions:  $\text{PhSH}$ , Eosin, Py, hexane, 540 nm, 40 °C, 5h (without alkyne).

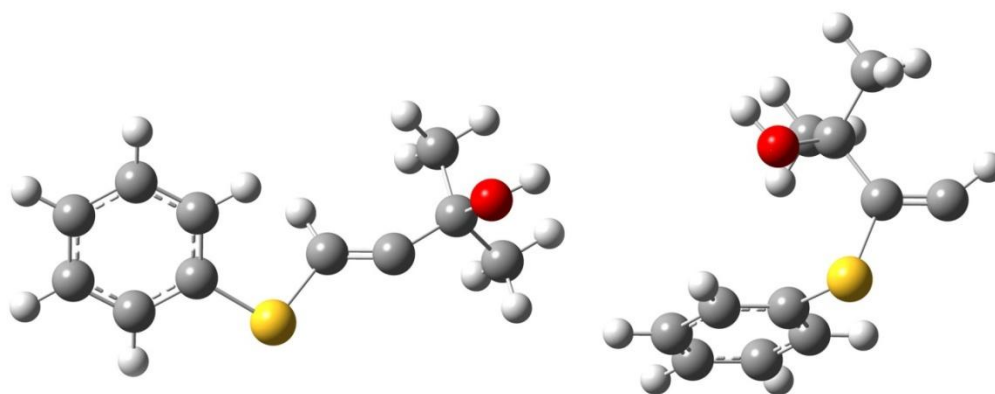
Trapping PhS<sup>•</sup> radical by the alkyne has shown the same trend as illustrated by the experiments shown in **Table S7**. Trace level of the product without Eosin (**Table S7**, entries 1, 2), product formation in the presence of Eosin (**Table S7**, entry 3) and good product yield in the presence of air due to regeneration of the dye (**Table S7**, entry 4). Trapping of the PhS<sup>•</sup> radical by alkyne is much more efficient process as compared to recombination, therefore larger yields were observed. Nevertheless, the overall tendency remained the same (cf. **Table S6** and **S7**).

**Table S7.** The yields of product **3a** in the photochemical reaction of the alkyne **1a** and PhSH without alkyne.<sup>a</sup>

Entry	Conditions	Yield of 3a, %
1	Without Eosin and without air	trace
2	Without Eosin and with air	trace
3	With Eosin and without air	18
4	With Eosin and with air	85

<sup>a</sup> Conditions: PhSH, alkyne, Eosin, Py, hexane, 540 nm, 40 °C, 5h.

### Calculated relative stability of radical species



Radical bearing linear structure (left) was found more stable as compared to branched structure (right) by  $\Delta G = 8.4$  kcal/mol as calculated at B3LYP/cc-pVTZ level (see Scheme 4B for structures; Ar = C<sub>6</sub>H<sub>5</sub>, R = CMe<sub>2</sub>OH).

Geometry optimization and frequency calculations were carried out at B3LYP/cc-pVTZ level using a standard basis set (Gaussian 09 program).

#### **S4. Construction of a photochemical reactor using 3D printing**

Initial prerequisites to the design of the reactor were: 1) the ability to easily install and remove LEDs in standard star-shaped enclosure without soldering; 2) accommodation of common glass vials available in the lab; 3) access of ambient air to the reaction mixture; 4) the ability to heat or cool the reaction mixture. In order to satisfy these demands, the following prototype was created (Figure S2). The reactor has the shape of a 28-mm high cylinder. The vial is inserted from the bottom and fixed with the O-ring fitted into the 3 mm groove. The vial is inserted up to the lower edge of the ventilation holes, located in the upper part of the reactor. The twelve ventilation holes have diameter of 3 mm are located on the outer surface of the reactor (Figure S2, section D-D). The plate dividing the vial and LED compartments is located just above the ventilation holes. The central hole in the plate was designed to fit the lens of the LED mounted on top. The remaining holes (Figure S2, section C-C) are used to pass-through the power supply wires. The wires are inserted through the opposite holes and wrapped around another O-ring, which is fitted into the groove in the upper part of the reactor. The LED is placed on top of the assembly and fixed via rotation until it is fixed with four clamps (Figure S2, section B-B). Upon rotation the contact pads of the LED are aligned with the power supply holes and the wire is pressed against the pad with the O-ring engaging the electrical contact. The assembly sequence is depicted in **Figure S3**.

We used standard 2 mL glass vials (14x50 mm) for the photochemical reactions. The vials were covered with aluminum tape to reduce the light loss. It is important to note that fixing the vial with the O-ring allows using slightly different vials ( $\pm 1$  mm in diameter) without any modifications. If the vessel with significantly different geometry should be used, the new reactor with altered dimensions can be printed in a matter of minutes.

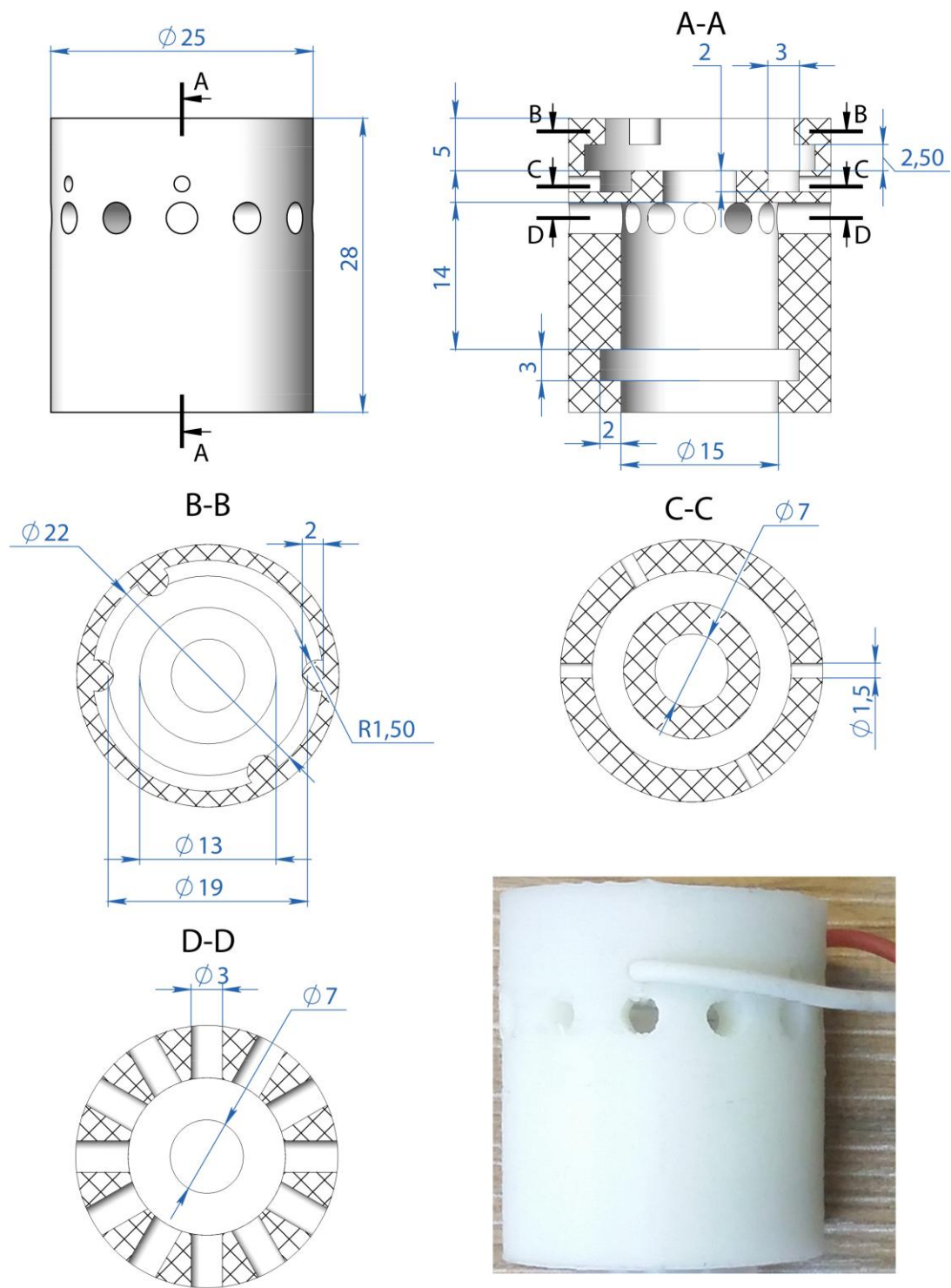


**Figure S2.** Drawings of the photoreactor. Front view (top left) and cut views for the specified planes (A-A, B-B, C-C, D-D). Bottom right – the photograph of the assembled reactor. All sizes are given in mm.

The reactor was printed from the 3 mm white ABS filament using Picaso Designer 250 FDM printer. The model was sliced in 0.2 mm layers using Slic3r software with parameters modified to speed up printing. Nozzle temperature was set to 260 (230) °C for the first and all remaining layers, respectively. Heated bed plate temperature was set to 110 (90) °C. The total print time was 20-30 minutes, depending on the exact geometry. About 6 grams of plastic were used to print a single part. The reactor was powered with a low-cost 12V to 5V/300 mA buck driver circuit as a power supply. In principle, any current source providing up to 300 mA is sufficient.

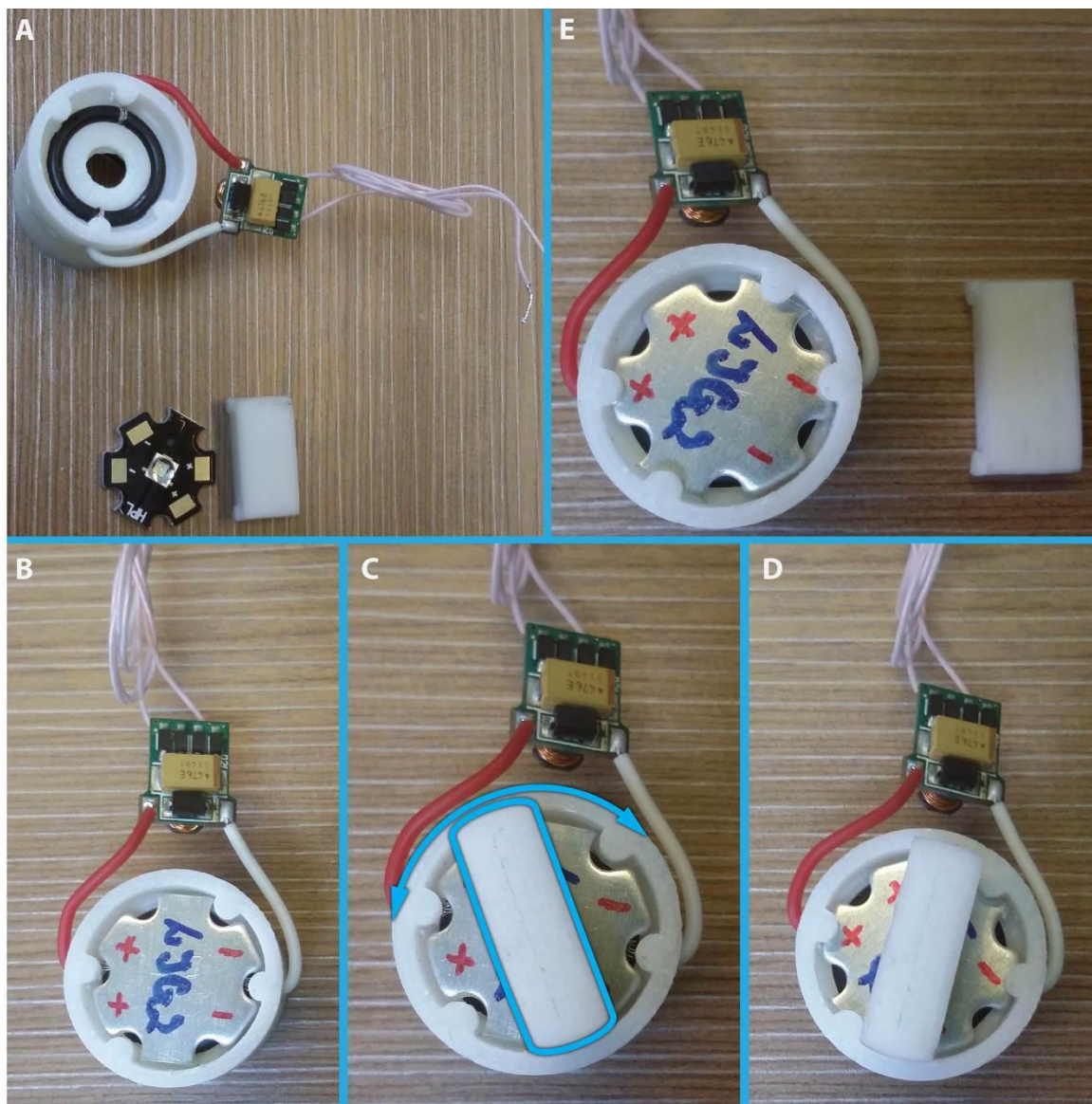


**Figure S3.** LED installation procedure. A – general view of the reactor, the LED and the key used to fix the LED; B – the LED is placed into the reactor; C – the LED is rotated with the key against the stop; D – the LED becomes fixed with the clamps; E – the key is removed, the reactor is ready to use.

## S5. Characterization of products 3a-p

### *(E)*-2-methyl-4-(phenylthio)-but-3-en-2-ol (**3a**)

$^1\text{H}$  NMR ( $\text{CDCl}_3$ , 500 MHz): 7.37 (2H, d, 7 Hz), 7.32 (2H, t, 7 Hz), 7.24 (1H, tt,  $J = 7$  Hz, 1Hz), 6.43 (1H, d,  $J = 15.2$  Hz), 6.03 (1H, d,  $J = 15.2$  Hz), 1.84 (1H, br.s), 1.37 (6H, s).  $^{13}\text{C}\{^1\text{H}\}$  NMR ( $\text{CDCl}_3$ , 125 MHz): 140.8, 135.4, 129.6, 129.2, 126.8, 120.9, 71.4, 29.9. The product was identified according to the published data.<sup>2</sup>

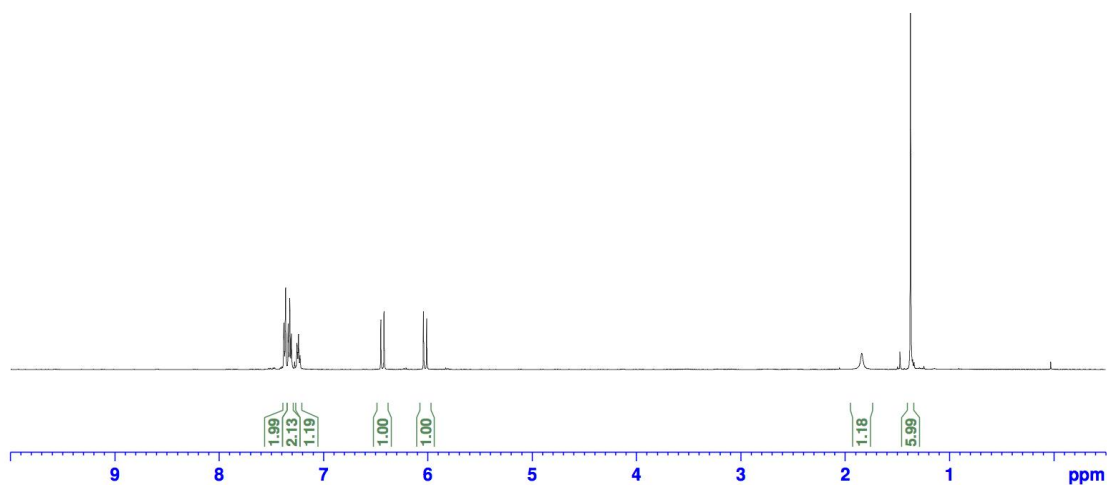


Figure S4.  $^1\text{H}$  NMR spectrum of **3a**

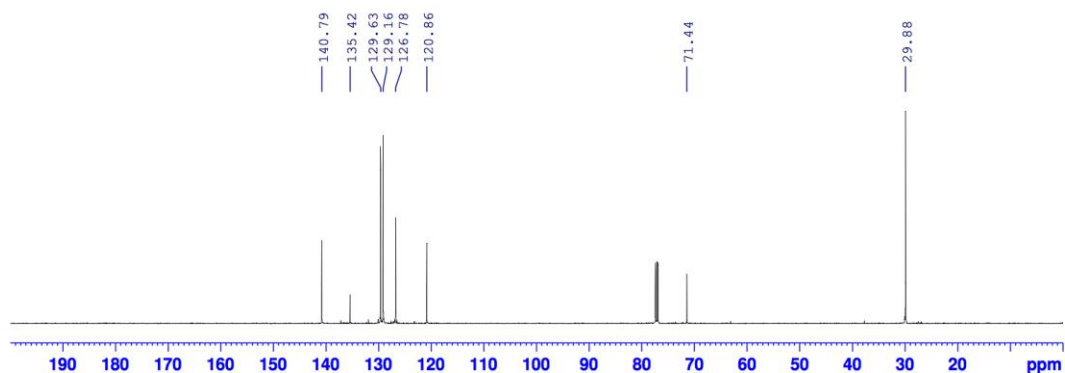


Figure S5.  $^{13}\text{C}\{^1\text{H}\}$  NMR spectrum of **3a**

### *(E)*-4-((2-bromophenyl)thio)-2-methylbut-3-en-2-ol (**3b**)

$^1\text{H}$  NMR (acetone- $d_6$ , 500 MHz): 7.58 (1H, d,  $J = 7$  Hz), 7.31-7.38 (2H, m), 7.12 (1H, td,  $J = 8$  Hz, 3 Hz), 6.46 (1H, d,  $J = 15.0$  Hz), 6.30 (1H, d,  $J = 15.0$  Hz), 3.93 (1H, s), 1.34 (6H, s).  $^{13}\text{C}\{^1\text{H}\}$  NMR (acetone- $d_6$ , 125 MHz) 148.5, 139.2, 133.7, 128.8, 127.9, 122.1, 117.3, 71.2, 30.2. Anal. calcd

(%) for C<sub>11</sub>H<sub>13</sub>BrOS: C, 48.36; H, 4.80; Br, 29.25; S, 11.74. Found (%): C, 48.16; H, 4.92; Br, 28.60; S, 11.48. HRMS (ESI): Calcd for C<sub>11</sub>H<sub>13</sub>BrOS [M – OH] = 254.9838, found 254.9828 ( $\Delta$  = 3.9 ppm).

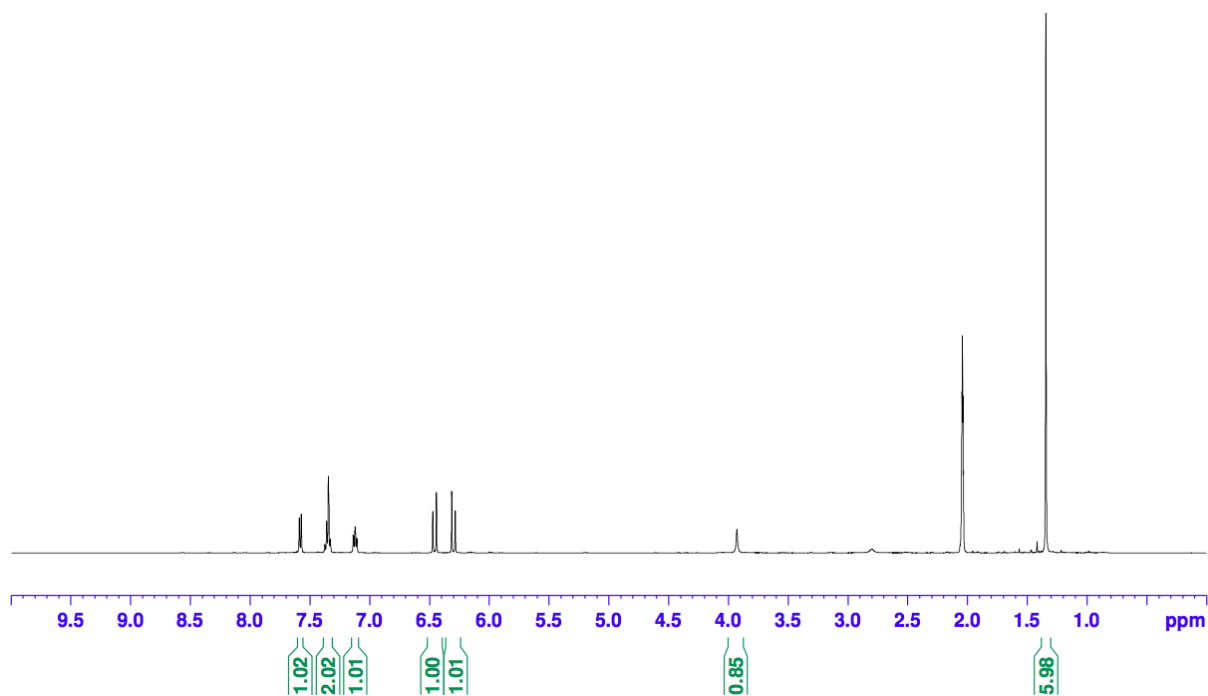


Figure S6. <sup>1</sup>H NMR spectrum of **3b**

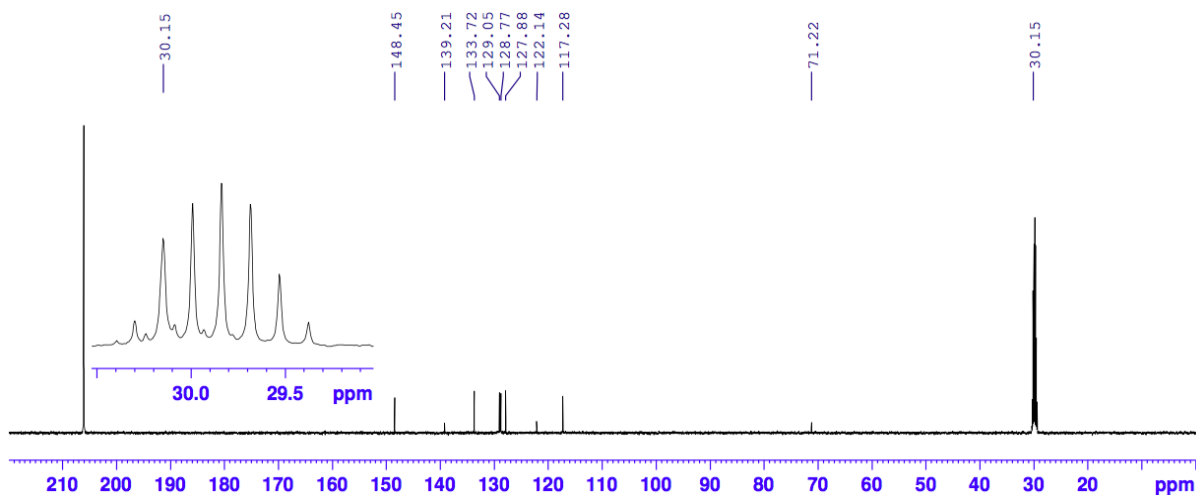


Figure S7. <sup>13</sup>C{<sup>1</sup>H} NMR spectrum of **3b**

*(E)*-4-((2-chlorophenyl)thio)-2-methylbut-3-en-2-ol (**3c**)

<sup>1</sup>H NMR (acetone-d<sub>6</sub>, 500 MHz): 7.43 (1H, dd, J = 8 Hz, 1 Hz), 7.37 (dd, 1H, J = 8 Hz, 2 Hz), 7.33 (1H, td, J = 8 Hz, 1 Hz), 7.22 (1H, td, J = 8 Hz, 2 Hz), 6.47 (1H, d, J = 15.0 Hz), 6.31 (1H, d, J =

15.0 Hz), 4.04 (1H, s), 1.36 (6H, s).  $^{13}\text{C}\{^1\text{H}\}$  NMR (acetone- $d_6$ , 125 MHz) 148.4, 137.1, 132.1, 130.4, 128.7, 128.5, 127.7, 116.7, 71.2, 30.1. Anal. calcd (%) for  $\text{C}_{11}\text{H}_{13}\text{ClOS}$ : C, 57.76; H, 5.73; Cl, 15.50; S, 14.02. Found (%): C, 57.03; H, 5.65; Cl, 15.06; S, 13.62. HRMS (ESI): Calcd for  $\text{C}_{11}\text{H}_{13}\text{ClOS} [\text{M} - \text{OH}] = 211.0343$ , found 211.0341 ( $\Delta = 0.9$  ppm).

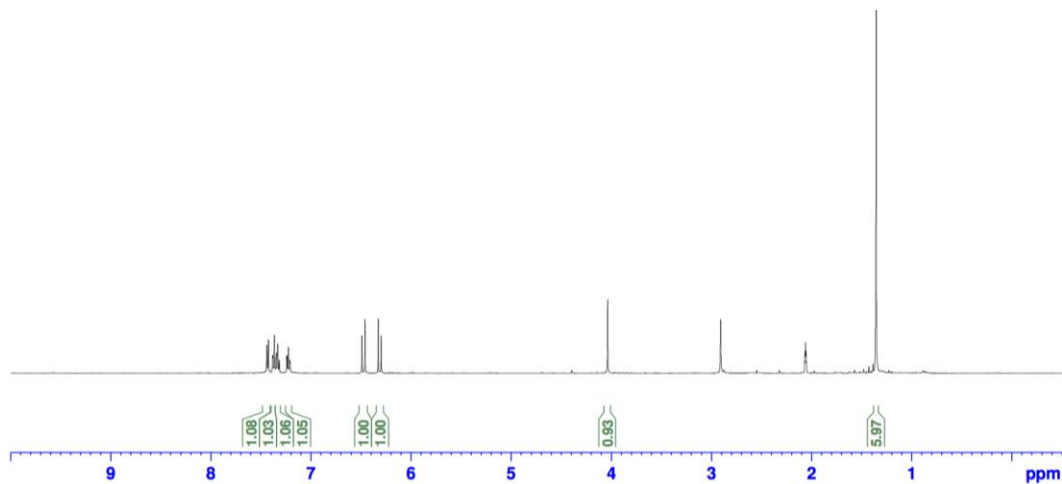


Figure S8.  $^1\text{H}$  NMR spectrum of **3c**

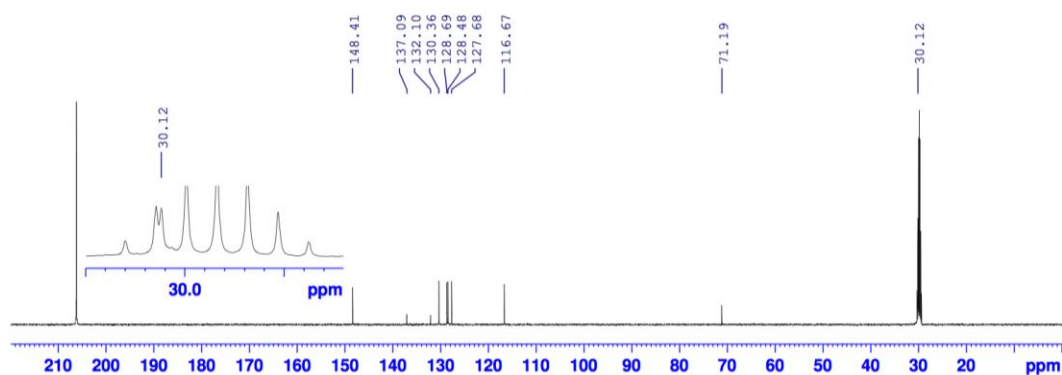


Figure S9.  $^{13}\text{C}\{^1\text{H}\}$  NMR spectrum of **3c**

*(E)*-4-((2-methoxyphenyl)thio)-2-methylbut-3-en-2-ol (**3d**)

$^1\text{H}$  NMR (acetone- $d_6$ , 500 MHz) 7.26 (1H, dd,  $J = 8$  Hz, 1 Hz), 7.21 (1H, td,  $J = 8$  Hz, 1 Hz), 6.99 (1H, d,  $J = 8$  Hz), 6.95 (1H, td,  $J = 8$  Hz, 1 Hz), 6.43 (1H, d,  $J = 15.4$  Hz), 6.13 (1H, d,  $J = 15.4$  Hz), 3.87 (3H, s), 3.81 (1H, s), 1.33 (6H, s).  $^{13}\text{C}\{^1\text{H}\}$  NMR (acetone- $d_6$ , 125 MHz) 157.3, 145.1, 128.8, 127.9, 125.8, 122.0, 118.3, 111.7, 71.1, 56.1, 30.3. Anal. calcd (%) for  $\text{C}_{12}\text{H}_{16}\text{O}_2\text{S}$ : C, 64.25; H,

7.19; S, 14.29. Found (%): C, 64.12; H, 7.00; S, 14.55. HRMS (ESI): Calcd for C<sub>12</sub>H<sub>16</sub>O<sub>2</sub>S [M – OH] = 207.0838, found 207.0835 ( $\Delta = 1.4$  ppm).

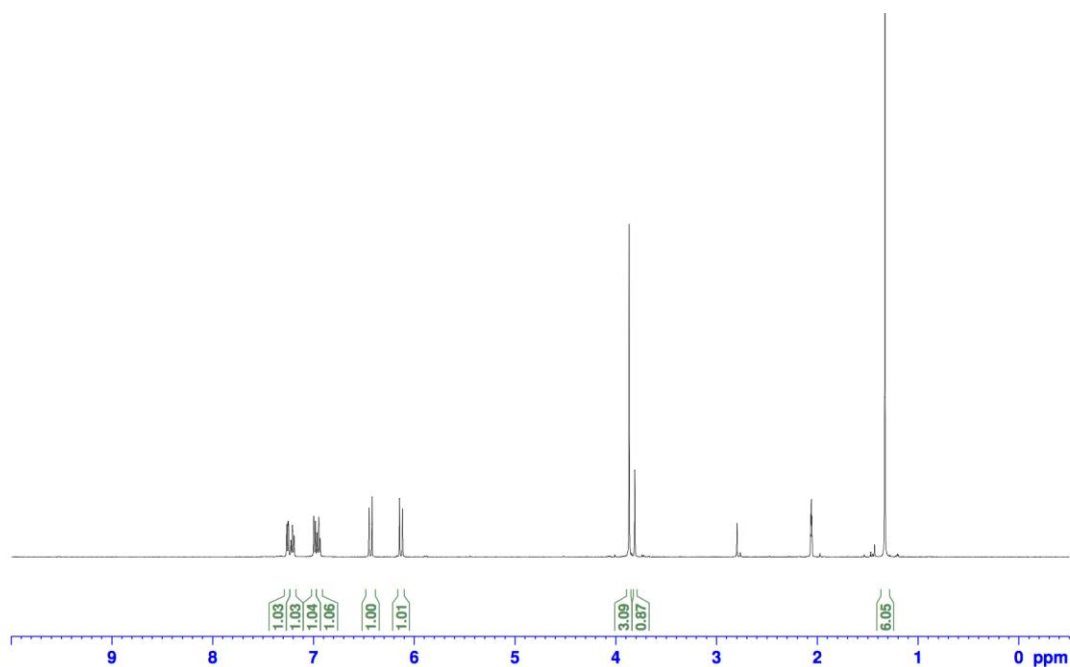


Figure S10. <sup>1</sup>H NMR spectrum of **3d**

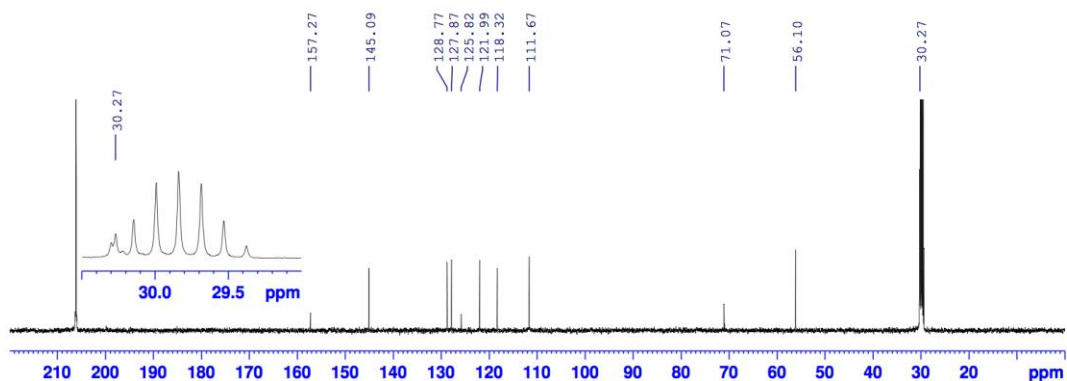


Figure S11. <sup>13</sup>C{<sup>1</sup>H} NMR spectrum of **3d**

*methyl (E)-2-((3-hydroxy-3-methylbut-1-en-1-yl)thio)benzoate (3e)*

<sup>1</sup>H NMR (acetone-d<sub>6</sub>, 500 MHz) 7.94 (1H, dd, J = 8 Hz, 1 Hz), 7.53 (1H, td, J = 8 Hz, 1 Hz), 7.46 (1H, d, J = 8 Hz), 7.27 (1H, td, J = 8 Hz, 1 Hz), 6.51 (1H, d, J = 15.3 Hz), 6.34 (1H, d, J = 15.3 Hz), 3.92 (1H, s), 3.89 (1H, s), 1.37 (6H, s). <sup>13</sup>C{<sup>1</sup>H} NMR (acetone-d<sub>6</sub>, 125 MHz) 167.0, 148.7,

142.3, 133.4, 131.8, 128.3, 127.7, 125.4, 118.5, 71.2, 52.3, 30.2. Anal. calcd (%) for C<sub>13</sub>H<sub>16</sub>O<sub>3</sub>S: C, 61.88; H, 6.39; S, 12.71. Found (%): C, 61.71; H, 6.35; S, 12.39. HRMS (ESI): Calcd for C<sub>13</sub>H<sub>16</sub>O<sub>3</sub>S [M – OH<sup>-</sup>] = 235.0787, found 235.0789 (Δ = 0.9 ppm).

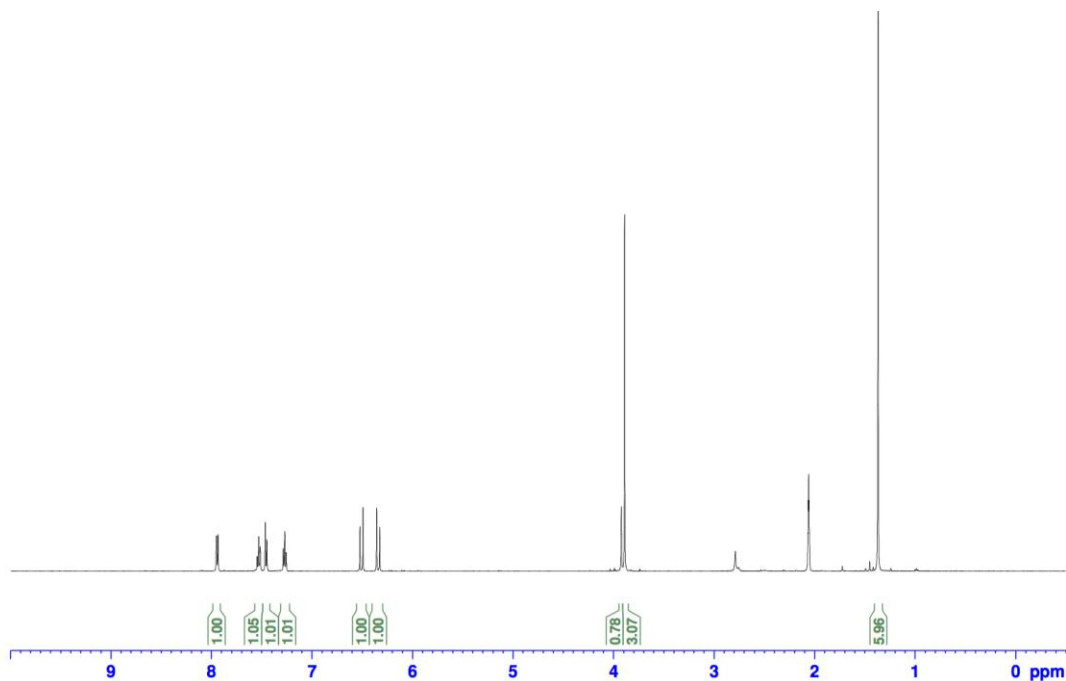


Figure S12. <sup>1</sup>H NMR spectrum of **3e**

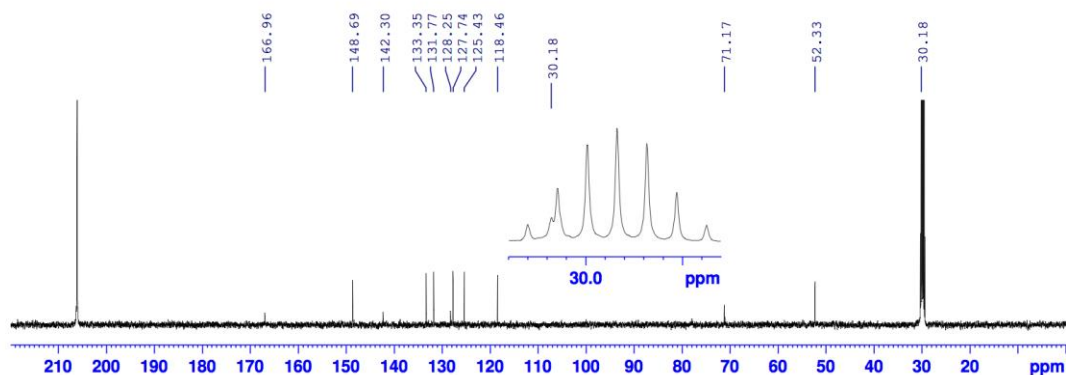


Figure S13. <sup>13</sup>C{<sup>1</sup>H} NMR spectrum of **3e**

*(E)*-4-((2,4-dimethylphenyl)thio)-2-methylbut-3-en-2-ol (**3f**)

<sup>1</sup>H NMR (acetone-d<sub>6</sub>, 500 MHz) 7.25 (1H, d, J = 7.9 Hz), 7.08 (1H, s), 7.02 (1H, d, J = 7.9 Hz), 6.32 (1H, d, J = 15.1 Hz), 5.86 (1H, d, J = 15.1 Hz), 3.74 (1H, s), 2.32 (3H, s), 2.29 (3H, s), 1.29 (6H,

s).  $^{13}\text{C}\{^1\text{H}\}$  NMR (acetone- $d_6$ , 125 MHz) 141.8, 138.9, 137.8, 132.0, 131.4, 131.3, 128.3, 120.1, 71.0, 30.3, 20.9, 20.3. Anal. calcd (%) for  $\text{C}_{13}\text{H}_{18}\text{OS}$ : C, 70.23; H, 8.16; S, 14.42. Found (%): C, 70.20; H, 7.95; S, 14.45. HRMS (ESI): Calcd for  $\text{C}_{13}\text{H}_{18}\text{OS}$   $[\text{M} - \text{OH}] = 205.1045$ , found 205.1045 ( $\Delta = 0.0$  ppm).

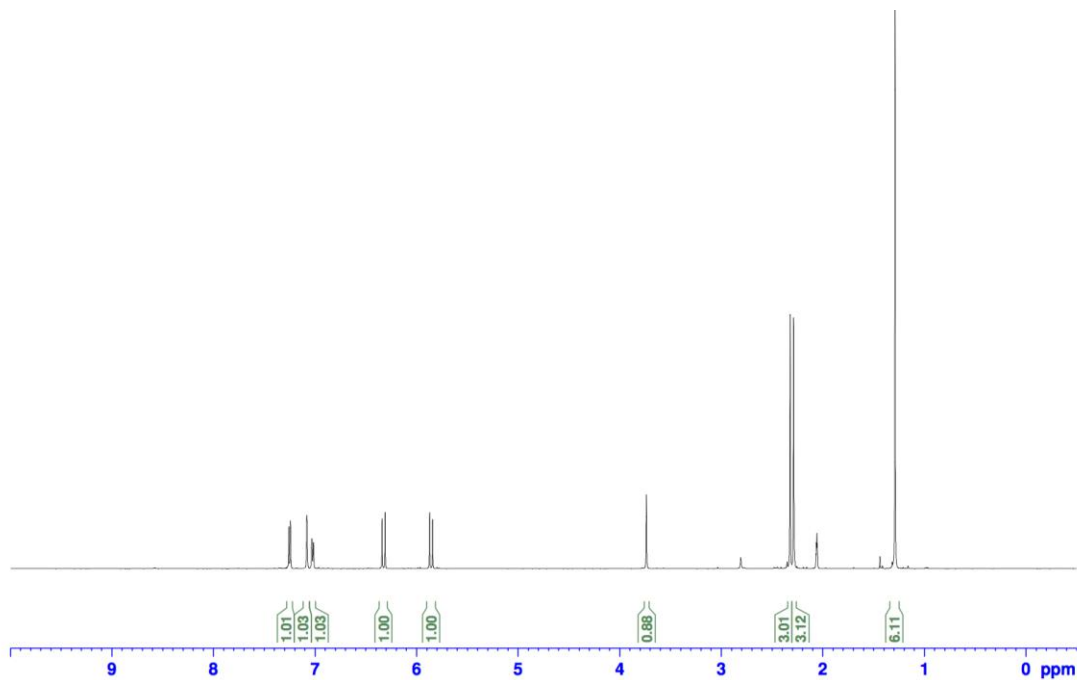


Figure S14.  $^1\text{H}$  NMR spectrum of **3f**

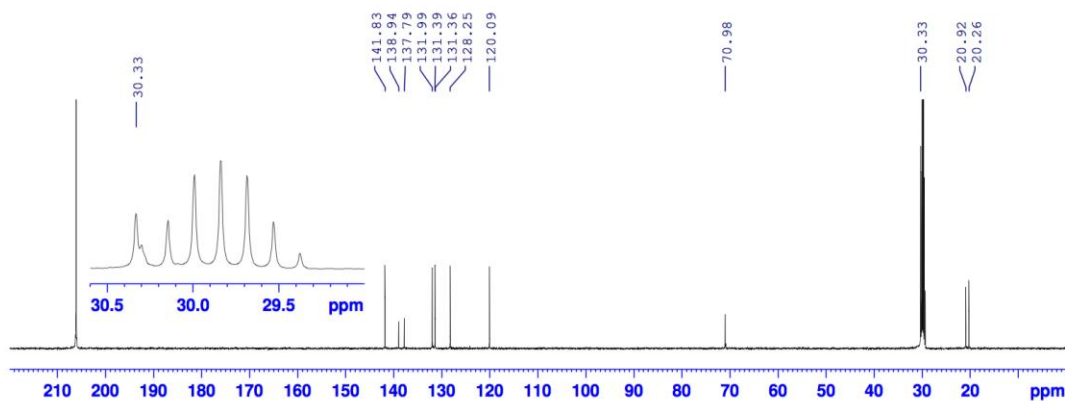


Figure S15.  $^{13}\text{C}\{^1\text{H}\}$  NMR spectrum of **3f**

*(E)*-2-methyl-4-((2-(trifluoromethyl)phenyl)thio)but-3-en-2-ol (**3g**)

$^1\text{H}$  NMR (acetone- $d_6$ , 500 MHz) 7.72 (1H, d,  $J = 8$  Hz), 7.60 (1H, t,  $J = 8$  Hz), 7.57 (1H, d,  $J = 8$  Hz), 7.40 (1H, t,  $J = 8$  Hz), 6.45 (1H, d,  $J = 15.0$  Hz), 6.28 (1H, d,  $J = 15.0$  Hz), 3.92 (1H, s), 1.34 (6H, s).  $^{13}\text{C}\{^1\text{H}\}$  NMR (acetone- $d_6$ , 125 MHz) 148.1, 137.3, 133.5, 130.9, 128.5 (q,  $J_{\text{CF}} = 30.0$  Hz), 127.6 (q,  $J_{\text{CF}} = 5.7$  Hz), 127.0, 125.0 (q,  $J_{\text{CF}} = 273.4$  Hz), 117.7, 71.2, 30.1. Anal. calcd (%) for  $\text{C}_{12}\text{H}_{13}\text{F}_3\text{OS}$ : C, 54.95; H, 5.00. Found (%): C, 54.60; H, 5.18. HRMS (ESI): Calcd for  $\text{C}_{12}\text{H}_{13}\text{F}_3\text{OS} [\text{M} - \text{OH}^-] = 245.0606$ , found 245.0606 ( $\Delta = 0.0$  ppm).

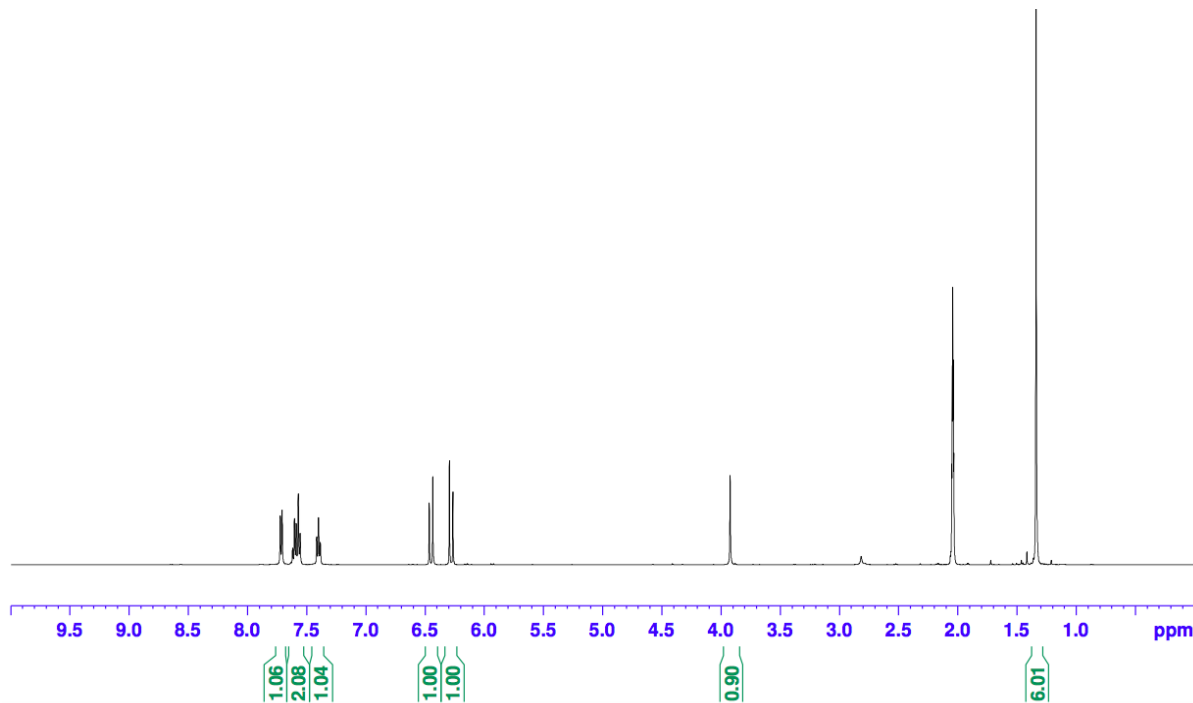


Figure S16.  $^1\text{H}$  NMR spectrum of **3g**

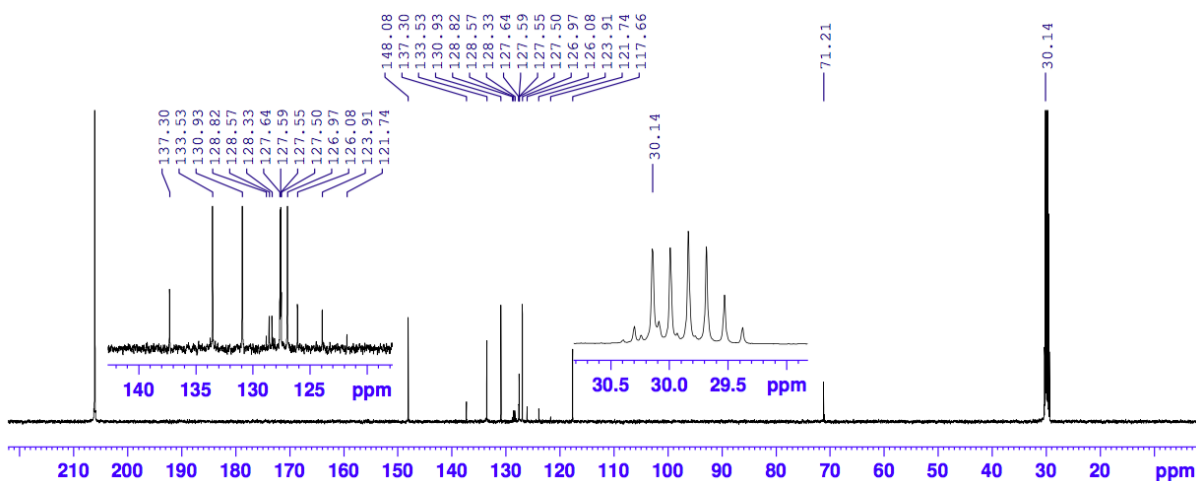


Figure S17.  $^{13}\text{C}\{^1\text{H}\}$  NMR spectrum of **3g**

*(E)*-2-methyl-4-((4-(trifluoromethyl)phenyl)thio)but-3-en-2-ol (**3h**)

$^1\text{H}$  NMR (acetone- $d_6$ , 500 MHz) 7.65 (2H, d,  $J = 8$  Hz), 7.50 (2H, d,  $J = 8$  Hz), 6.54 (1H, d,  $J = 15.2$  Hz), 6.31 (1H, d,  $J = 15.2$  Hz), 3.99 (1H, s), 1.35 (6H, s).  $^{13}\text{C}\{^1\text{H}\}$  NMR (acetone- $d_6$ , 125 MHz) 147.3, 142.8, 127.1, 127.0 (q,  $J_{\text{CF}} = 32.6$  Hz), 125.8 (q,  $J_{\text{CF}} = 3.7$  Hz), 125.5, 124.5 (q,  $J_{\text{CF}} = 270.8$  Hz), 115.8, 70.3, 29.3. Anal. calcd (%) for  $\text{C}_{12}\text{H}_{13}\text{F}_3\text{OS}$ : C, 54.95; H, 5.00. Found (%): C, 54.83; H, 5.12. HRMS (ESI): Calcd for  $\text{C}_{12}\text{H}_{13}\text{F}_3\text{OS}$  [ $\text{M} - \text{OH}$ ] = 245.0606, found 245.0608 ( $\Delta = 0.8$  ppm)

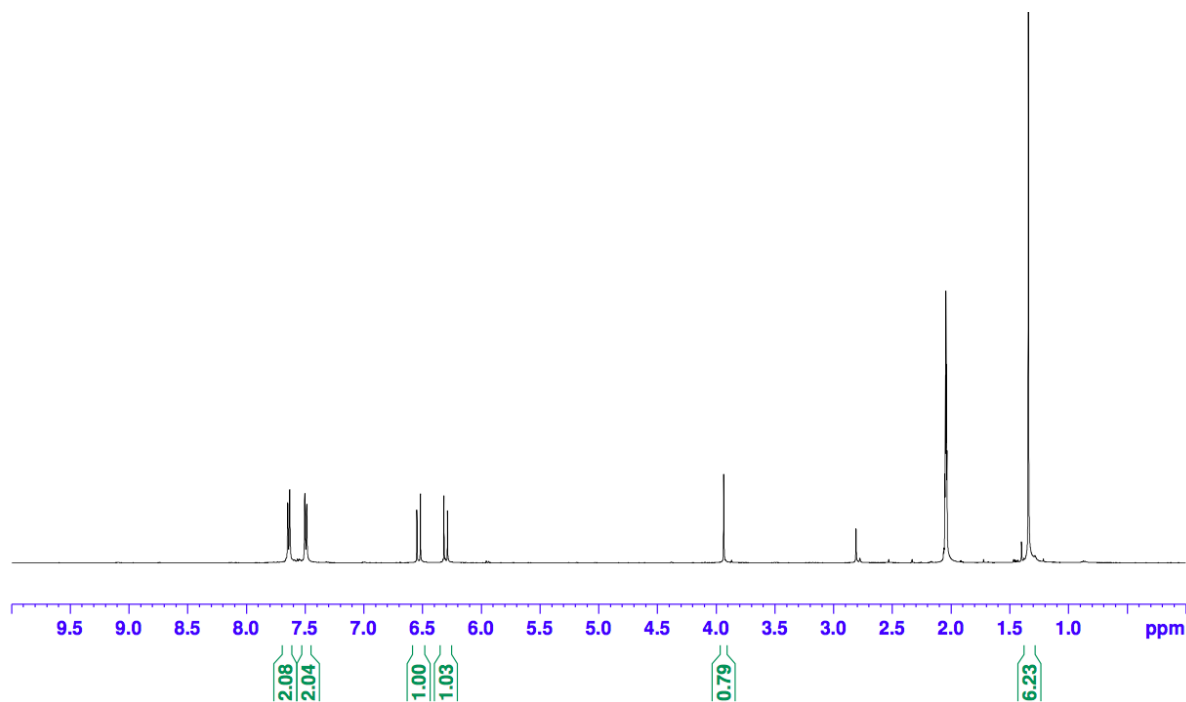


Figure S18.  $^1\text{H}$  NMR spectrum of **3h**



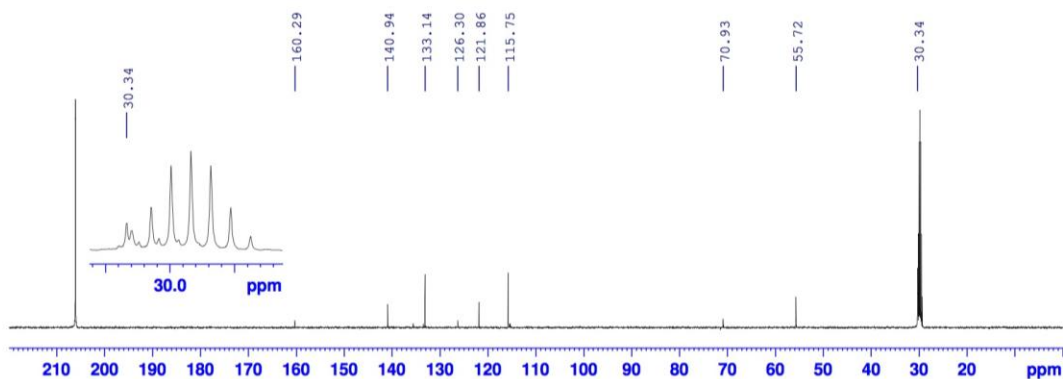


Figure S21.  $^{13}\text{C}\{^1\text{H}\}$  NMR spectrum of **3i**

*(E)*-4-((4-chlorophenyl)thio)-2-methylbut-3-en-2-ol (**3j**)

$^1\text{H}$  NMR (acetone- $d_6$ , 500 MHz) 7.35 (2H, d,  $J = 9$  Hz), 7.32 (2H, d,  $J = 9$  Hz), 6.43 (1H, d,  $J = 15.1$  Hz), 6.14 (1H, d,  $J = 15.1$  Hz), 3.85 (1H, s), 1.30 (6H, s).  $^{13}\text{C}\{^1\text{H}\}$  NMR (acetone- $d_6$ , 125 MHz) 145.6, 136.3, 132.5, 130.6, 130.0, 118.6, 71.1, 30.2. Anal. calcd (%) for  $\text{C}_{11}\text{H}_{13}\text{ClOS}$ : C, 57.76; H, 5.73; Cl, 15.50; S, 14.02. Found (%): C, 57.61; H, 5.84; Cl, 15.81; S, 13.22. HRMS (ESI): Calcd for  $\text{C}_{11}\text{H}_{13}\text{ClOS}$  [ $\text{M} - \text{OH}$ ] = 211.0343, found 211.0339 ( $\Delta = 1.9$  ppm).

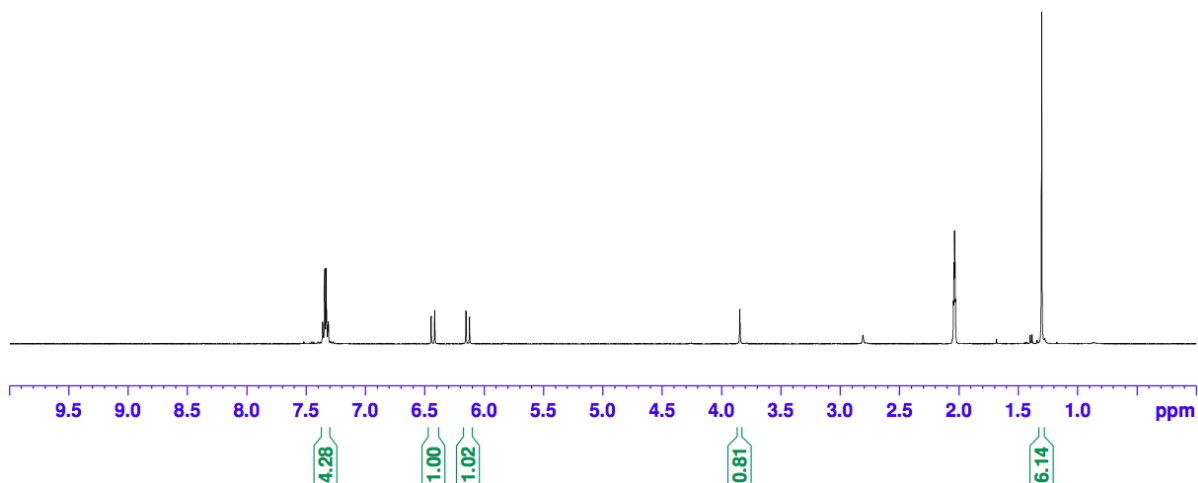


Figure S22.  $^1\text{H}$  NMR spectrum of **3j**

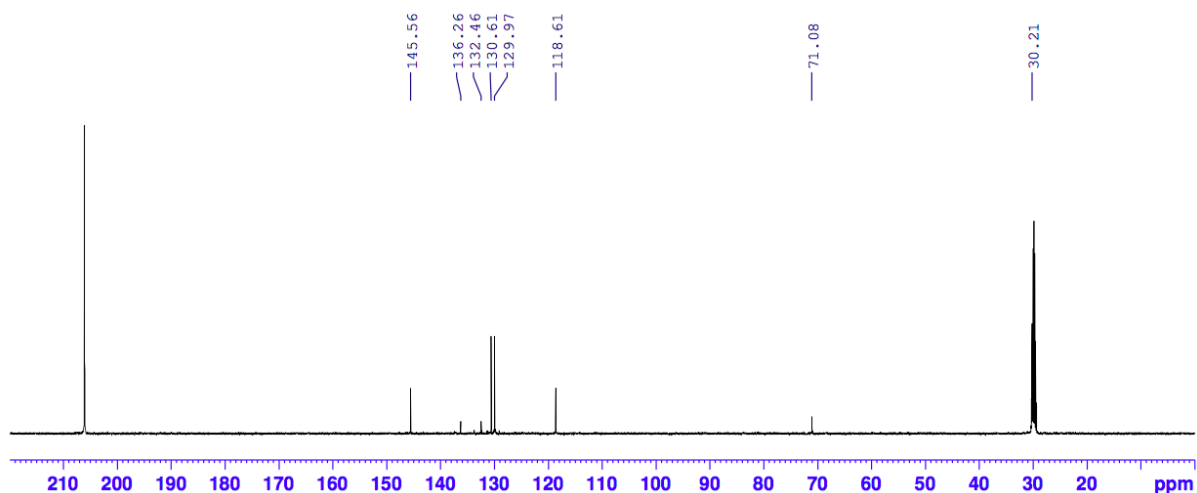


Figure S23.  $^{13}\text{C}\{^1\text{H}\}$  NMR spectrum of **3j**

*(E)*-2-methyl-4-(*p*-tolylthio)but-3-en-2-ol (**3k**)

$^1\text{H}$  NMR (acetone- $d_6$ , 500 MHz) 7.25 (2H, d,  $J = 8.1$ ), 7.18 (2H, d,  $J = 8.1$ ), 6.41 (1H, d,  $J = 15.2$  Hz), 6.02 (1H, d,  $J = 15.2$  Hz), 3.77 (1H, s), 2.31 (3H, s), 1.30 (6H, s).  $^{13}\text{C}\{^1\text{H}\}$  NMR (acetone- $d_6$ , 125 MHz) 142.9, 137.2, 133.1, 130.7, 130.1, 120.3, 71.0, 30.3, 21.0. Anal. calcd (%) for  $\text{C}_{12}\text{H}_{16}\text{OS}$ : C, 69.19; H, 7.74; S, 15.39. Found (%): C, 69.31; H, 7.77; S, 15.22. HRMS (ESI): Calcd for  $\text{C}_{12}\text{H}_{16}\text{OS}$  [ $\text{M} - \text{OH}^-$ ] = 191.0889, found 191.0888 ( $\Delta = 0.5$  ppm).

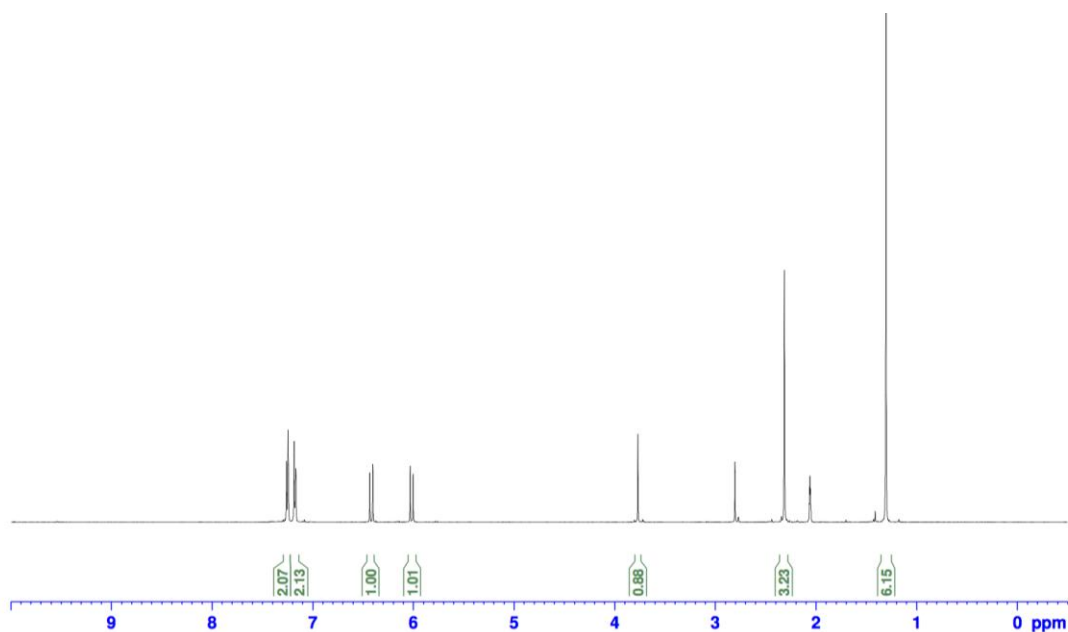


Figure S24.  $^1\text{H}$  NMR spectrum of **3k**

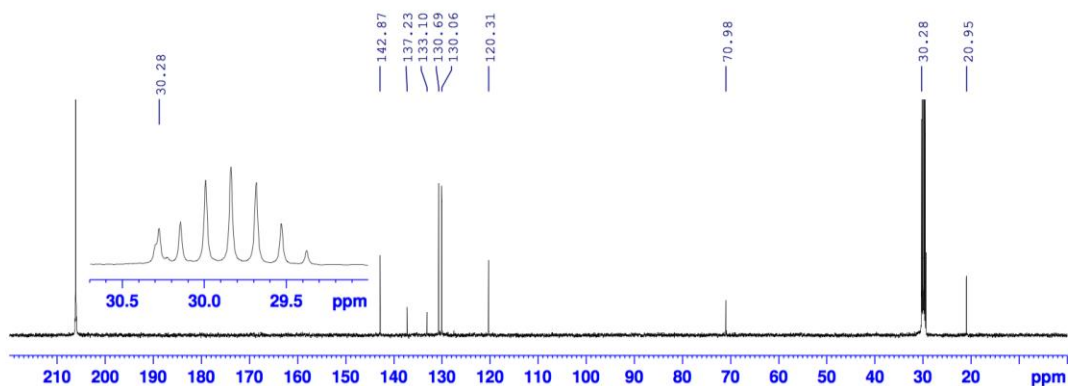


Figure S25.  $^{13}\text{C}\{^1\text{H}\}$  NMR spectrum of **3k**

*(E)*-4-((3-chlorophenyl)thio)-2-methylbut-3-en-2-ol (**3l**)

$^1\text{H}$  NMR (acetone- $d_6$ , 500 MHz) 7.36 (1H, t,  $J = 7.8$  Hz), 7.32 (1H, t,  $J = 1.8$  Hz), 7.28 (1H, dt,  $J = 7.8$  Hz,  $\sim 1.5$  Hz), 7.25 (1H, dt,  $J = 7.8$  Hz,  $\sim 1.5$  Hz), 6.49 (1H, d,  $J = 15.1$  Hz), 6.23 (1H, d,  $J = 15.1$  Hz), 3.92 (1H, s), 1.34 (6H, s).  $^{13}\text{C}\{^1\text{H}\}$  NMR (acetone- $d_6$ , 125 MHz) 146.8, 140.0, 135.3, 131.4, 127.8, 126.9, 126.8, 117.7, 71.13, 30.2. Anal. calcd (%) for  $\text{C}_{11}\text{H}_{13}\text{ClOS}$ : C, 57.76; H, 5.73; Cl, 15.50; S, 14.02. Found (%): C, 57.58; H, 5.77; S, 14.22. HRMS (ESI): Calcd for  $\text{C}_{11}\text{H}_{13}\text{ClOS}$  [ $\text{M} - \text{OH}$ ] = 211.0343, found 211.0339 ( $\Delta = 1.9$  ppm).

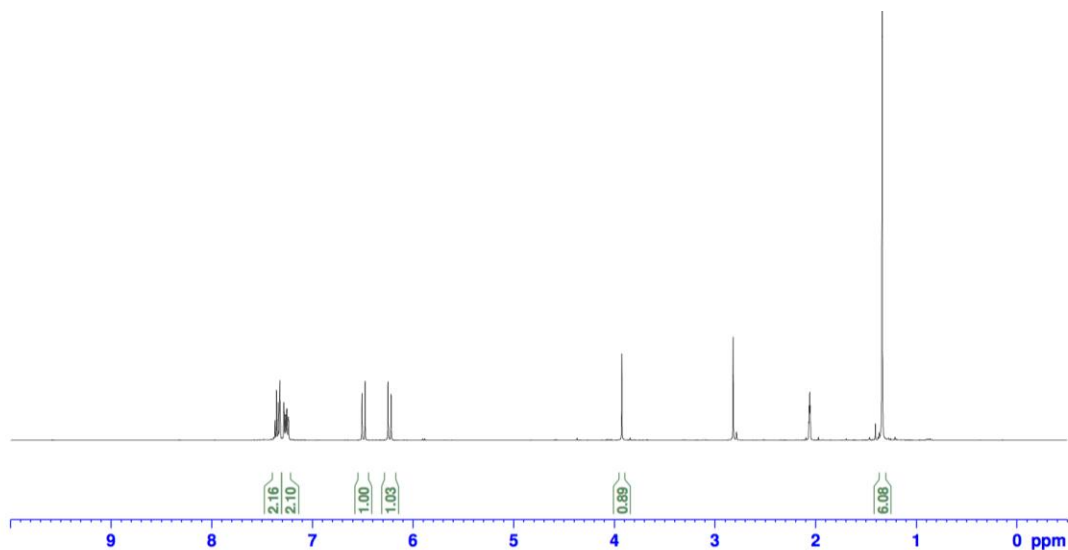


Figure S26.  $^1\text{H}$  NMR spectrum of **3l**

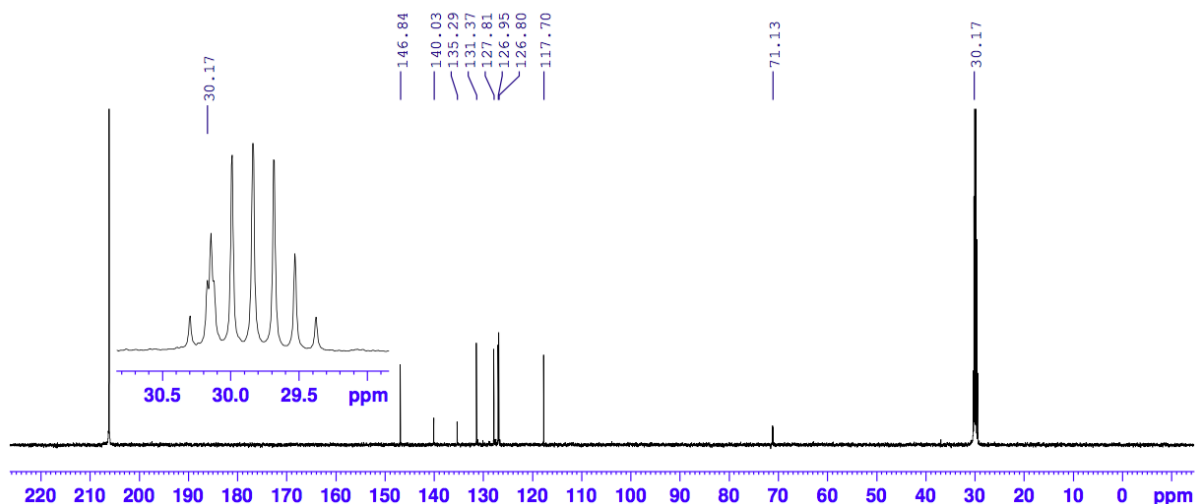


Figure S27.  $^{13}\text{C}\{^1\text{H}\}$  NMR spectrum of **3I**

*(E)*-4-((3,5-dimethylphenyl)thio)-2-methylbut-3-en-2-ol (**3m**)

$^1\text{H}$  NMR (acetone- $d_6$ , 500 MHz) 6.96 (2H, s), 6.87 (1H, s), 6.45 (1H, d,  $J = 15.1$  Hz), 6.08 (1H, d,  $J = 15.1$  Hz), 3.83 (1H, s), 2.27 (3H, s), 1.31 (6H, s).  $^{13}\text{C}\{^1\text{H}\}$  NMR (acetone- $d_6$ , 125 MHz) 143.5, 139.5, 136.5, 128.9, 126.9, 119.7, 71.0, 30.3, 21.2. Anal. calcd (%) for  $\text{C}_{13}\text{H}_{18}\text{OS}$ : C, 70.23; H, 8.16; S, 14.42. Found (%): C, 70.40; H, 7.99; S, 14.58. HRMS (ESI): Calcd for  $\text{C}_{13}\text{H}_{18}\text{OS}$  [ $\text{M} - \text{OH}$ ] = 205.1045, found 205.1046 ( $\Delta = 0.5$  ppm).

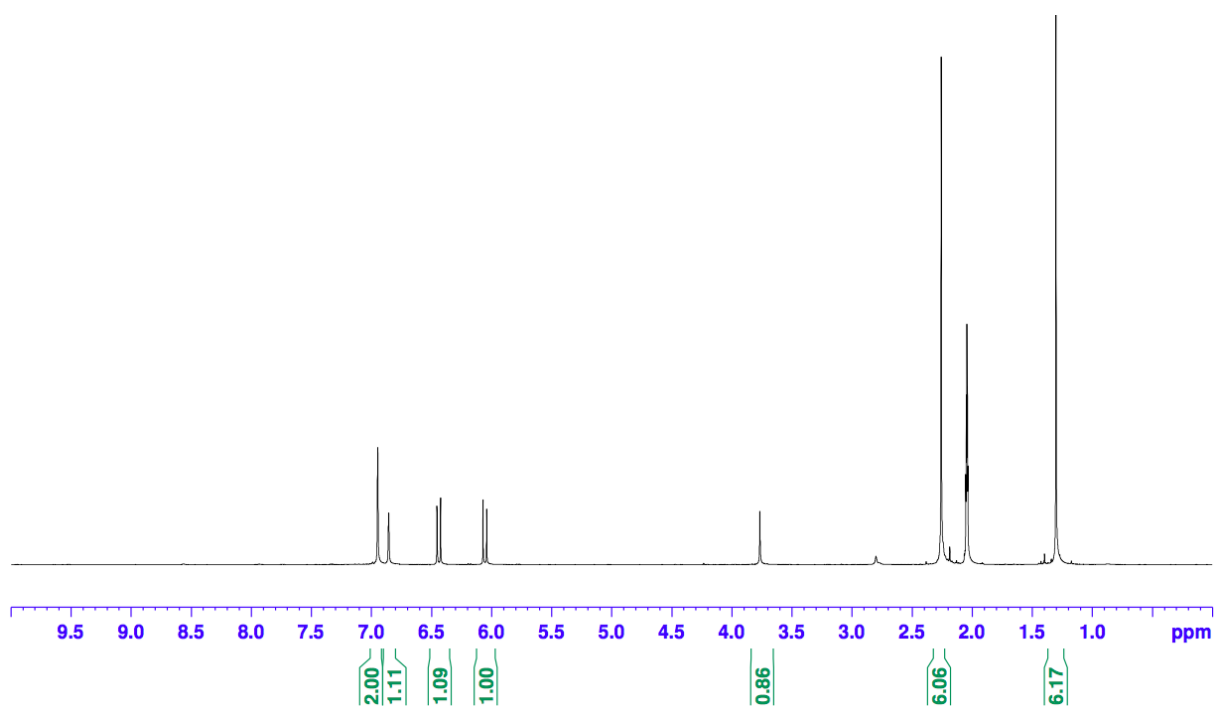


Figure S28.  $^1\text{H}$  NMR spectrum of **3m**

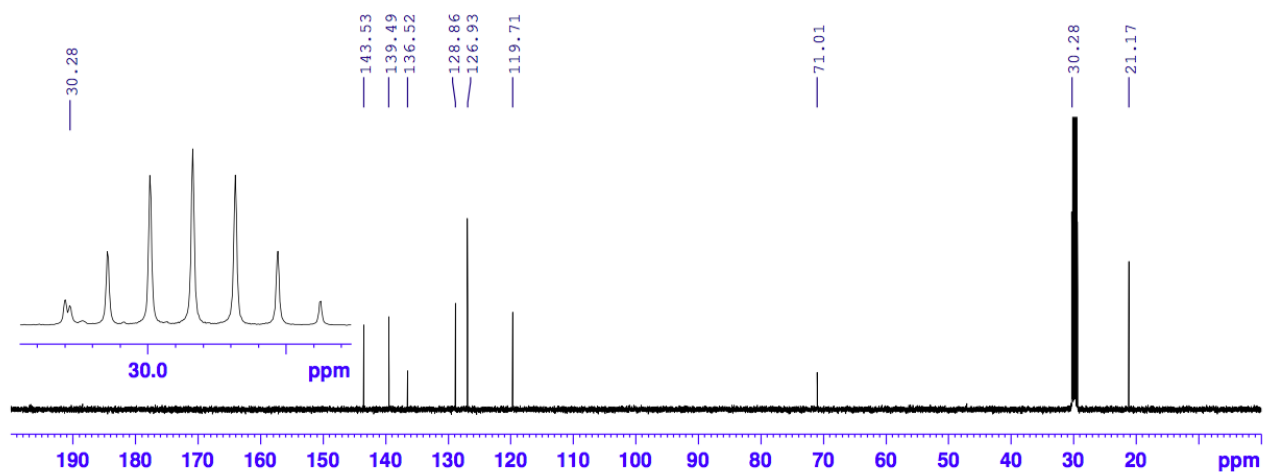


Figure S29.  $^{13}\text{C}\{^1\text{H}\}$  NMR spectrum of **3m**

*(E)*-1-(2-(phenylthio)vinyl)cyclohexan-1-ol (**3n**)

$^1\text{H}$  NMR (acetone- $d_6$ , 500 MHz): 7.33-7.36 (4H, m), 7.23 (1H, m), 6.50 (1H, d,  $J = 15.1$  Hz), 6.11 (1H, d,  $J = 15.1$  Hz), 3.57 (1H, s), 1.67-1.79 (2H, m), 1.44-1.66 (7H, m), 1.24-1.36 (1H, m).

$^{13}\text{C}\{^1\text{H}\}$  NMR (acetone- $d_6$ , 125 MHz): 144.4, 137.2, 130.0, 129.3, 127.1, 120.1, 72.0, 38.6, 26.3, 22.6.

The product was identified according to the published data.<sup>3</sup>

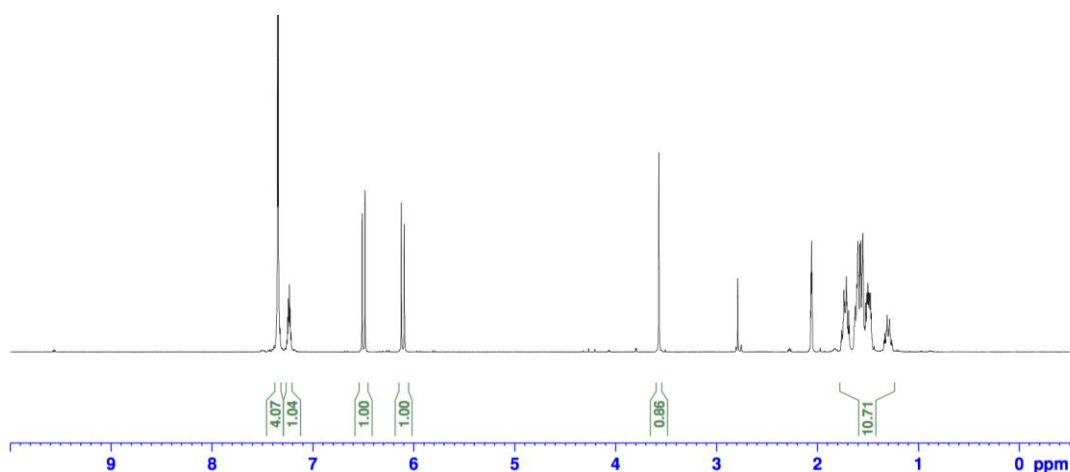


Figure S30.  $^1\text{H}$  NMR spectrum of **3n**

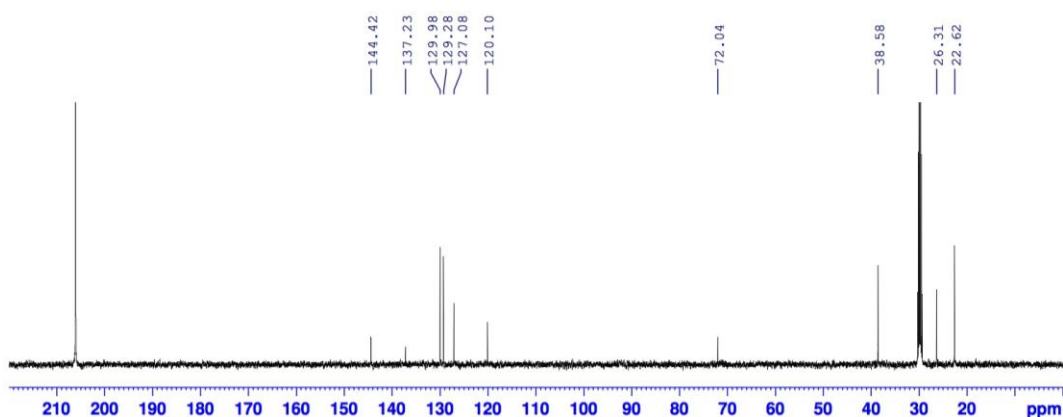


Figure S31.  $^{13}\text{C}\{^1\text{H}\}$  NMR spectrum of **3n**

*(E)*-3,4,4-trimethyl-1-(phenylthio)pent-1-en-3-ol (**3o**)

$^1\text{H}$  NMR (acetone- $d_6$ , 500 MHz): 7.34-7.37 (4H, m), 7.24 (1H, m), 6.49 (1H, d,  $J = 15.0$  Hz), 6.20 (1H, d,  $J = 15.0$  Hz), 3.64 (1H, s), 1.30 (3H, s), 0.98 (9H, s).  $^{13}\text{C}\{^1\text{H}\}$  NMR (acetone- $d_6$ , 125 MHz): 141.5, 137.3, 129.9, 129.2, 127.0, 120.6, 77.6, 38.3, 25.8, 23.9. Anal. calcd (%) for  $\text{C}_{14}\text{H}_{20}\text{OS}$ : C, 71.14; H, 8.53; S, 13.56. Found (%): C, 71.31; H, 8.77; S, 13.22. HRMS (ESI): Calcd for  $\text{C}_{14}\text{H}_{20}\text{OS}$   $[\text{M} - \text{OH}]^- = 219.1202$ , found 219.1197 ( $\Delta = 2.3$  ppm).

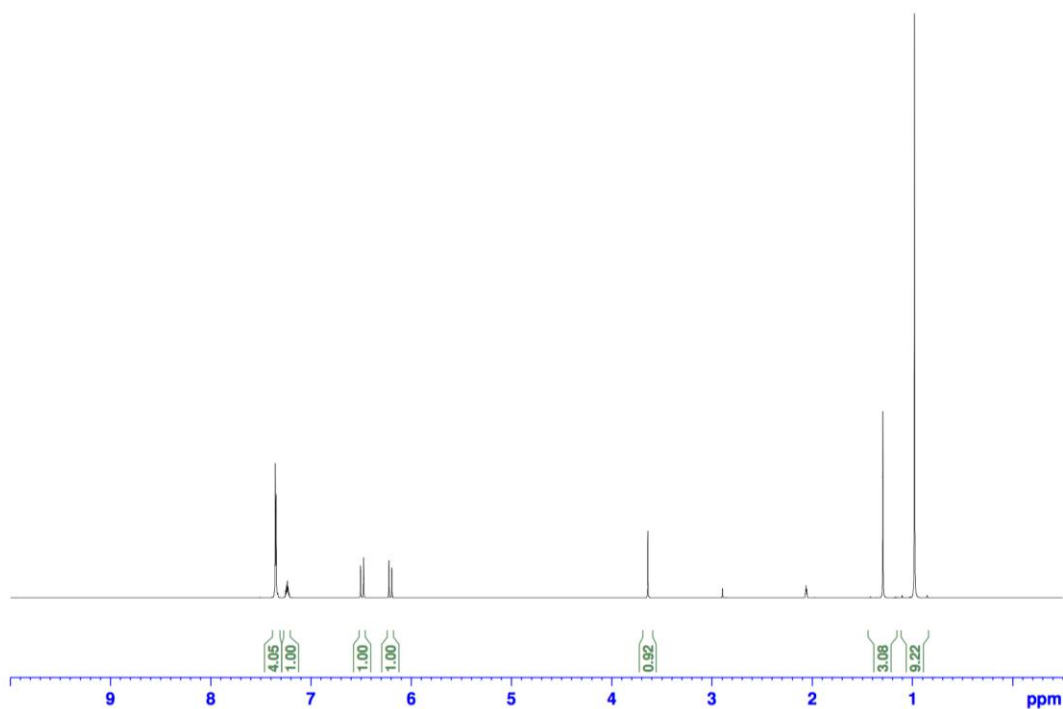


Figure S32.  $^1\text{H}$  NMR spectrum of **3o**

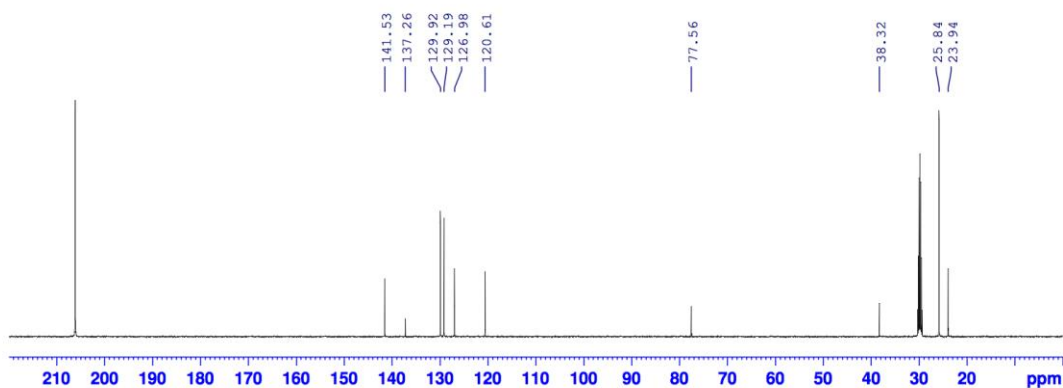


Figure S33.  $^{13}\text{C}\{^1\text{H}\}$  NMR spectrum of **3o**

*(E)*-1,1-diphenyl-3-(phenylthio)prop-2-en-1-ol (**3p**)

$^1\text{H}$  NMR (acetone- $d_6$ , 500 MHz) 7.40-7.44 (4H, m), 7.29-7.37 (8H, m), 7.20-7.26 (3H, m), 6.59 (1H, d,  $J = 15.1$  Hz), 6.50 (1H, d,  $J = 15.1$  Hz), 5.07 (1H, s).  $^{13}\text{C}\{^1\text{H}\}$  NMR (acetone- $d_6$ , 125 MHz) 146.7, 139.1, 135.5, 129.2, 129.0, 128.5, 127.9, 126.8, 126.7, 122.5, 78.7. Anal. calcd (%) for

C<sub>21</sub>H<sub>18</sub>OS: C, 79.21; H, 5.70; S, 10.07. Found (%): C, 79.01; H, 5.59; S, 10.20. HRMS (ESI): Calcd for C<sub>21</sub>H<sub>18</sub>OS [M – OH<sup>-</sup>] = 301.1045, found 301.1047 (Δ = 0.7 ppm).

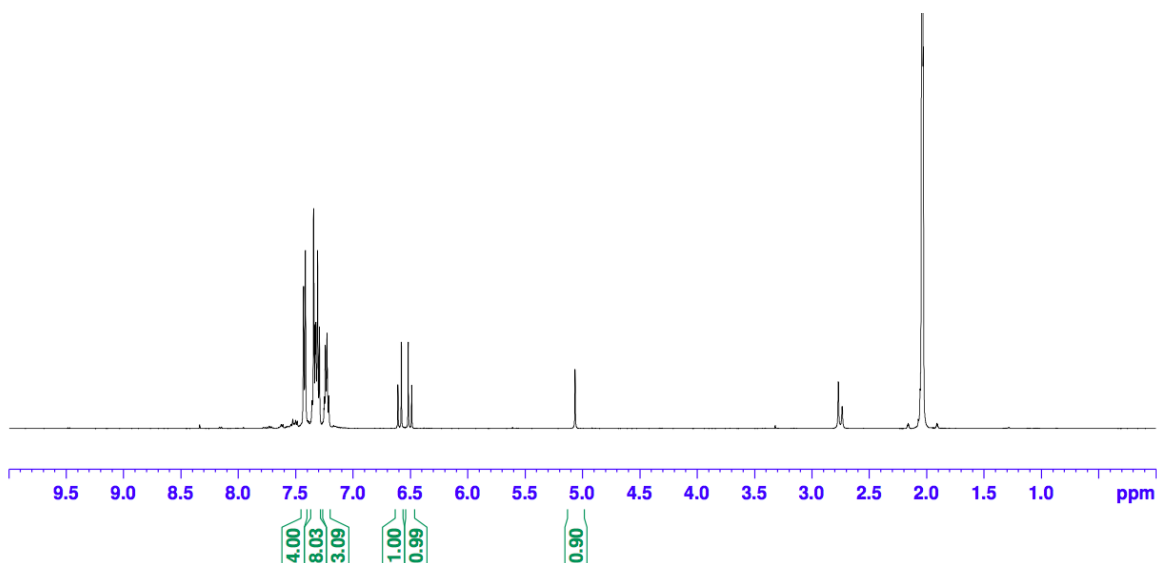


Figure S34. <sup>1</sup>H NMR spectrum of **3p**

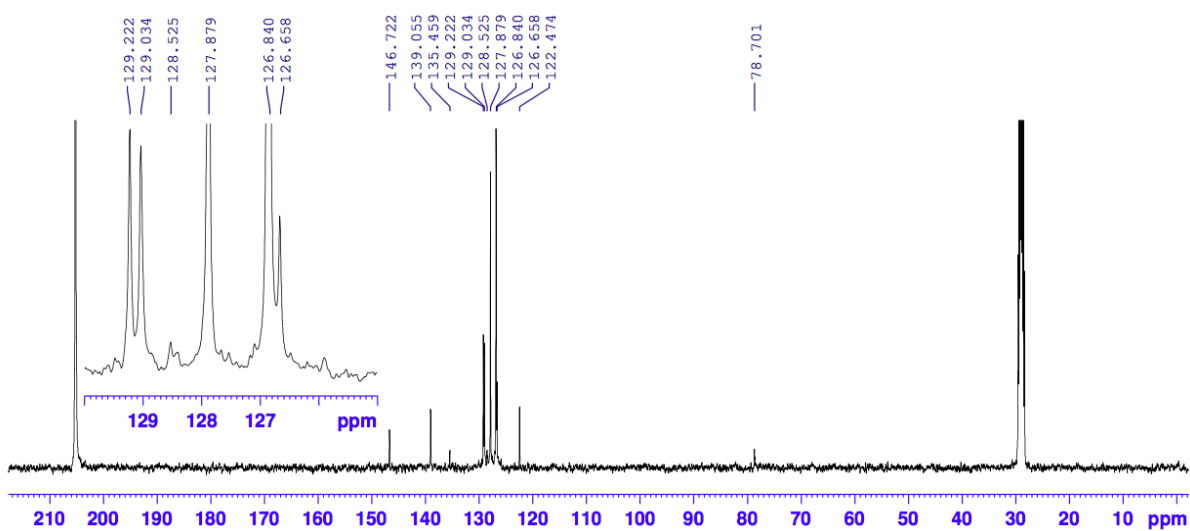


Figure S35. <sup>13</sup>C{<sup>1</sup>H} NMR spectrum of **3p**

## References

---

- <sup>1</sup> Yoshida, J.; Nakatani, S.; Ise, S. *J. Org. Chem.* **1993**, *58*, 4855.
- <sup>2</sup> Silva, M. S.; Lara, R. G.; Marczewski, J. M.; Jacob, R. G.; Lenardao, E. J.; Perin, G. *Tetrahedron Lett.* **2008**, *49*, 1927.
- <sup>3</sup> Guerrero Jr., P. G.; Dabdoub, M. J.; Marques, F. A.; Wosch, C. L.; Baroni, A. C. M.; Ferreira, A. G. *Synth. Commun.* **2008**, *38*, 24, 4379.